PAPER NAME
233-1456-2-CE_check.docx

AUTHOR
Samsul Bahri

WORD COUNT
4512 Words

CHARACTER COUNT
25344 Characters

PAGE COUNT
13 Pages

FILE SIZE
628.1KB

SUBMISSION DATE
Nov 20, 2022 10:53 AM GMT+7

REPORT DATE
Nov 20, 2022 10:54 AM GMT+7

19% Overall Similarity

The combined total of all matches, including overlapping sources, for each database.

- 10% Internet database
- 17% Publications database
- Crossref database
- Crossref Posted Content database
- 7% Submitted Works database

Excluded from Similarity Report

- Bibliographic material
- Cited material

GLOBAL OPTIMIZATION VERY FAST SIMULATED ANNEALING INVERSION FOR THE INTERPRETATION OF GROUNDWATER POTENTIAL

OPTIMASI GLOBAL INVERSI VERY FAST SIMULATED ANNEALING UNTUK INTERPRETASI POTENSI AIR TANAH

Samsul Bahri[1]*, Sanny Virginia Aponno[2], Zulfiah[2]

[1]Departement of Geophysical Engineering, University of Pattimura
[2]Departement of Geological Engineering, University of Pattimura

Keywords:
Groundwater Potential, Vertical Electrical Sounding, Very Fast Simulated Annealing, Global Optimization

Corespondent Email:
Samsul.bahri@fatek.unpatti.ac.id

Abstract. This study examines the inversion modelling of one-dimensional Schlumberger configuration resistivity data using the Very Fast Simulated Annealing (VFSA). Detailed identification and mapping of aquifer conditions is very important for the sustainable development of groundwater resources in an area. Vertical electrical sounding (VES) and surface electrical resistivity surveys have proven very useful for studying groundwater due to their simplicity and cost effectiveness. Global optimization inversion method also provides an inversion solution that is not expected to be trapped in a local minimum solution, so that it will get results that are closer to the actual situation. The VFSA method is inspired by phenomena in metallurgy related to the formation of crystals in materials caused by thermodynamic processes. This inversion scheme was tested initially with free noise synthetic data and with noise 5%. Furthermore, the program is applied to field data that has been measured in Ambon City, Maluku, Indonesia. The results of the VFSA inversion on field data obtained four layers consisting of top soil (141.2 $\pm$ 0,6 Ωm) with a thickness of 1.43 m, andesite breccia rock (355.90 $\pm$ 0.46 m) with a thickness of 4 m, lapilli tuff (93.40 $\pm$ 0.31 m) with 30 m thick, then the last is the coarse tuff layer (34.30 $\pm$ 0.15 m) which is estimated as an aquifer.

Abstrak. *Penelitian ini mengkaji pemodelan inversi data resistivitas konfigurasi Schlumberger satu dimensi menggunakan teknik Very Fast Simulated Annealing (VFSA). Identifikasi dan pemetaan secara detail terkait kondisi akuifer sangat penting untuk pembangunan berkelanjutan sumber daya air tanah suatu daerah. Vertical electrical sounding (VES) dan survei resistivitas listrik permukaan telah terbukti sangat berguna untuk mempelajari air tanah karena kesederhanaan dan efektifitas biayanya. Metode optimasi global juga memberikan solusi inversi yang diharapkan tidak terjebak pada solusi minimum lokal, sehingga akan mendapatkan hasil yang lebih mendekati keadaan sebenarnya. Metode VFSA terinspirasi dari fenomena di bidang metalurgi terkait pembentukan kristal dalam material yang disebabkan oleh proses termodinamika. Skema inversi ini dilakukan uji awal dengan data sintetik bebas gangguan dan*

dengan gangguan 5%. Selanjutnya program diterapkan pada data lapangan yang telah dilakukan di Kota Ambon, Maluku, Indonesia. Hasil inversi VFSA pada data lapangan diperoleh empat lapisan yang terdiri atas top soil (141,2 ± 0.61 Ωm) setebal 1,43 m, batuan andesite breccia (355,90 ± 0,46 Ωm) setebal 4 m, lapilli tuff (93,40 ± 0,31 Ωm) setebal 30 m, kemudian yang terakhir ialah lapisan coarse tuff (34,30 ± 0,15 Ωm) yang diperkirakan sebagai akuifer.

1. INTRODUCTION

Water is the most crucial need for all living things, especially for humans. The issue of clean water quality and sanitation is a worldwide concern and is included in the sustainable development goals program. In general, clean water is produced from groundwater exploration. Unfortunately, the high demand for groundwater due to industrialization and population growth has resulted in excessive groundwater exploitation. This is a major concern to maintain a sustainable aquifer condition. Detailed identification and mapping of aquifer conditions are very important for the sustainable development of groundwater resources in an area. Geophysical techniques are powerful tools and play an important role in delineating the configuration of subsurface aquifers. Over the last few years, modelling techniques related to this have developed a lot. In particular, the vertical electrical sounding (VES) technique and surface electrical resistivity survey has proven to be very useful for studying groundwater due to their simplicity and cost-effectiveness. Steiner try to applied resistivity methods combined with seismic methods to investigate pollutants in groundwater (Steiner et al., 2022). Besides that, the resistivity method can also be used to identify groundwater potential (Joel et al., 2020), especially in areas that are still hard to get clean water supply or areas that require agricultural irrigation (Alarifi et al., 2022; Chikabvumbwa et al., 2021; Zaher et al., 2021). The difference in resistivity values due to the presence of salt minerals such as sodium chloride in the aquifer can also be used to analyze the phenomenon of seawater intrusion using this method (Ammar et al., 2021; Wilopo et al., 2018).

Geoelectrical inversion problems are often non-linear and complex, where the solution consists of using a set of apparent resistivity data to obtain subsurface model parameters. There are two ways to do this (inverse modelling), there are direct and indirect methods. The indirect inverse modelling method involves curve matching and forward modelling algorithms. VES data interpretation with this technique is widely used by practitioners of hydrogeology. The direct inverse modelling method (ie resistivity inversion with a numerical algorithm) involves minimizing the error between the observed apparent resistivity and that calculated using optimization techniques. Commonly used techniques are the Ridge Regression Technique (Meju, 1992; Narayan et al., 1994), Joint Inversion (Özyıldırım et al., 2020), and the singular value decomposition (SVD) technique (Tjong et al., 2018). The revolutionary and newly developed optimization techniques are genetic algorithms, simulated annealing, and particle swarm optimization (Hapsoro et al., 2021; Yan et al., 2020). This method is also known as the global optimization method, where this method is more reliable and has a better error value because it does not get stuck on a local minimum.

The problem of inverse modelling of DC current resistivity was first investigated in the 1930s. From that time until the late 1980s, the field survey methodology and the character of the data from the measurements did not change much. Then in the late 1980s and early 1990s to this day, there has been a significant increase in data collection and interpretation. The interpretation of VES data is greatly influenced by three events, there is the linear filter theory proposed by Ghosh (Ghosh, 1971), the widespread use of digital computers, and the application of general linear inversion theory. At this time, the concept of inverse modelling and automated analysis is becoming popular,

where the computational program generated from this theory can find the most suitable model automatically.

In this study, we will discuss the inversion of the one-dimensional Schlumberger configuration resistivity data using the VFSA Technique. The advantage of VFSA over other methods is that it can get the global minimum solution and it can prevent the local minimum from being reached. VFSA inversion ensure the solution's stability and can be used to make the noise data robust. This technique can be used in geophysical inversion problems such as seismic (Wang et al., 2021), DC resistivity (Sharma, 2012), Self Potential (Biswas & Sharma, 2014), and electromagnetic time domain (Srigutomo et al., 2021).

2. LITERATURE REVIEW

The Schlumberger configuration is very easy to use for surveying and is the most popular scheme for measuring DC resistivity sounding. The VES method injects direct electric current into the ground, which will produce a hemispherical equipotential state. The relationship between apparent resistivity and layer parameters is expressed in the form of a Hankel integral. Koefoed expressed the equation for the homogeneous and isotropic earth model as follows (Koefoed, 1979),

$$\rho_a(L) = L^2 \int_0^\infty T(\lambda) J_1(\lambda L)\, \lambda\, d\lambda \quad (1)$$

where L is half the current electrode distance (AB/2), J_1 is a first order Bessel function of the first kind, and λ indicate an integral variable. $T(\lambda)$ is a resistivity transformation function obtained from the recursion relationship,

$$T_i = \frac{T_{i+1} + \rho_i \tanh(\lambda h_i)}{1 + (T_{i+1} \tanh(\lambda h_i)/\rho_i)} \quad (2)$$

where m is the number of layers, ρ_i is rock resistivity and h_i is thickness of the i-th layer. Furthermore, the value of the transformation function is related to the filter coefficient to produce apparent resistivity (Bhattacharya & Patra, 1968; Ghosh, 1971). Guptasarma introduced a 19 point filter (ϕ_r) which can be used to calculate apparent resistivity (Guptasarma, 1982). This linearization filter method is considered to have a better accuracy value than the method proposed by Gosh before (Ghosh, 1971). The apparent resistivity value is

$$\rho_a(L) = \sum_1^\alpha \phi_r\, T(\lambda) \quad (3)$$

λ can be obtained from $\lambda_r = 10^{(a_r - \log L)}$. This equation is used to calculate the forward modelling response for DC resistivity sounding data.

3. METHODS

in this study we used a very fast simulated annealing method for subsurface resistivity inversion. The global minimum inversion of Simulated Annealing (SA) is inspired by a phenomenon in metallurgy related to the formation of crystals in materials caused by thermodynamic processes. In annealing, the material is heated until it melts into a liquid. The temperature is then slowly lowered (annealed) and controlled so that the materials freeze at energy states very close to the global minimum and become crystals. However, if the cooling process is carried out rapidly (quenching), the material will freeze at a local minimum. At high temperatures, the atoms move randomly and freely, given the high kinetic energy. The cooling process is carried out resulting in atoms that are initially free to move to find an optimal place, where the internal energy required to maintain its position is minimum. The geophysical inversion problem takes an analogy from this annealing event, where the temperature cooling process is represented by an iteration process to find the optimum solution. Liquids represent the model, and the energy of the system is analogous to a cost function or an error function (Sen & Stoffa, 2013).

The Boltzmann probability distribution function is used in SA to describe the relationship between the model probabilities m at temperature T, whose energy E is,

$$P(\boldsymbol{m_i}) = \frac{\exp\left(-\frac{E(\boldsymbol{m_i})}{kT}\right)}{\sum_{j \in S} \exp\left(-\frac{E(\boldsymbol{m_j})}{kT}\right)} \quad (4)$$

Where k is Boltzmann's constant, where in the future the value will be set to $k=1$. The control parameter T has the same dimensions as the system energy or the error function.

In its development, SA gets modifications to obtain more efficient results. Ingber was the first to introduce VFSA for two main reasons. First, in the NM-dimensional model space, each model parameter has a different range and has a different effect on the misfit or error function. So each model parameter must have a different level of disturbance from its current position (Ingber, 1989, 1993). Second, some existing SA algorithms are not capable of performing sufficiently elegant and fast calculations if the Cauchy random number is equal to the number of model parameters. Attempts to construct an NM-dimensional Cauchy distribution can be avoided by using the NM product of the 1D Cauchy distribution. In such a formulation, each model parameter has its own cooling schedule and sampling scheme in the model space. Ingber proposed a new probability distribution for modelling so that convergence can be achieved without a slow cooling schedule. Assuming m_i^k there is model parameter m_i in k-iteration where,

$$m_i^{min} \leq m_i^k \leq m_i^{max} \quad (5)$$

m_i^{min} and m_i^{max} are the minimum and maximum value of each model parameter.

At first, the model parameters (resistivity and thickness of each layer) are chosen randomly from the model space. Then forward modelling is carried out to get the response function in the form of pseudo resistivity data. The error or energy function can be obtained by comparing it with the resistivity data of the real model with the second norm formula (L_2) as follows,

$$L_2 = E_2 = \frac{1}{N}\sqrt{\sum_{i=1}^{N}\left(\rho_i^{obs} - \rho_i^{model}\right)^2} \quad (6)$$

The second norm (L_2) also known as the least square. While ρ_i^{obs} and ρ_i^{model} are the resistivity value of the observation and model response at point-i. The number of observation points is N data. In the $(k+1)$-iteration, the parameter values of the model get a small perturbation based on the following rules,

$$m_i^{k+1} = m_i^k + y_i\left(m_i^{max} - m_i^{min}\right) \quad (7)$$

with $y_i \in [-1,1]$ and $m_i^{min} \leq m_i^{k+1} \leq m_i^{max}$. After that the random number u_i is generated from uniform distribution $u_i \in [0,1]$. The value of y_i based on temperature in this iteration is,

$$y_i = sgn\left(u_i - \frac{1}{2}\right) T_i\left[\left(1 + \frac{1}{T_i}\right)^{|u_i - 1|} - 1\right] \quad (8)$$

Then a new model has been obtained. The error function is then resurrected using the previous forward modelling. If the new model's misfit error is smaller than the previous model's misfit error, then the new model's parameters can be accepted. However, if the misfit error of the new model is greater than the misfit error of the previous model, then a random number from 0 to 1 is generated and compared with the probability of acceptance of the model. If the probability of acceptance of the model is greater than a random number, the new model can be accepted, and conversely, the new model is rejected if the probability is smaller. The temperature in the iteration process will affect the probability value of model acceptance, where the smaller the temperature, the smaller the probability of model acceptance. The decrease in temperature is based on the following cooling schedule,

$$T_i(k) = T_{01}\exp(-c_1 k^{1/NM}) \quad (9)$$

k and c_1 are constants, whose values differ depending on the model parameters. T_{01} is the initial temperature and T_i is the update temperature. The initial temperature value depends on the size of the optimization of the objective function (Sharma, 2012).

4. INVERSION RESULT

4.1. Inversion Results Using Synthetic Data

Forward modelling calculations using filter theory produce synthetic pseudo resistivity data. This inversion step using synthetic data aims to determine the efficacy of program development before being used to identify subsurface conditions from the real data. The calculation of parameter values is carried out 10 times, then the best

model selection is taken from the mean result. The apparent resistivity data used is free noise and with 5% random noise. Giving noise aims to evaluate the performance of programming against real data. We use the parameter model in Ekinci and Demirci and compare it with the deterministic inversion damp least square inversion program with the Singular Value Decomposition (SVD) technique (Ekinci & Demirci, 2008). For the free noise synthetic data, we use a three-layer earth model with a Q-type data ($\rho_1 > \rho_2 > \rho_3$), with the inversion results as shown in **table 1**.

(Table 1. here)
(Fig 1. here)

The absence of noise results in the inversion results being similar to the actual value. From **Table 1**, it can be seen that the VFSA inversion gives a better error value than the conventional method. In **Fig. 1**, the pattern of misfit error decreases with the number of iterations. In the temperature reduction schedule the values of the constants c_1, k, and NM are set to 1. T_{01} is set to 5, this value is taken according to Srigutomo (2021) to obtain a rapid reduction of the error misfit. The application of a low initial temperature will have an impact on a low parameter selection probability value, as a result, no model parameter with a larger error is accepted as a solution. The inversion calculation was performed 10 times and the average value was taken. The number of iterations used is 2000 iterations. The results of the inversion using this scheme can be seen in **Fig. 2** and **Fig. 3**.

(Fig. 2 here)
(Fig. 3 here)

In general, there is always noise in the measurement of geophysical data, so the synthetic data is given a noise 5%. The model parameter data is based on Ekinci and Demirici (2008) for the QQ-type ($\rho_1 > \rho_2 > \rho_3 > \rho_4$) four-layer earth model. The inversion constant used is the same as in the previous step and the results are shown in **Table 2**. The uncertainty value depends on the magnitude of the model parameters and the order of the layers. The deeper the measurement, the uncertainty value tends to increase. It proves that rock resistivity measurements are less sensitive with increasing depth. The addition of the noise also affects the resistivity misfit error, although it is not significant.

(Table. 2 here)
(Fig. 4 here)

The pattern of decline in the objective function can be seen in **Fig. 4**, which is the same as before, no spikes in the objective function are received. In **Fig. 5** it can also be seen that the observation data and the calculated inversion data are quite close. Then in **Fig. 6**, it can be seen that there are differences in the distribution of resistivity at each depth in the model and the inversion results, where additional noise affects the efficacy of the VFSA inversion scheme, especially in deeper layers.

(Fig. 5 here)
(Fig. 6 here)

4.2. Inversion VFSA to the Field Data

The VFSA inversion scheme that has been tested before then can be applied to field data or real data. The resistivity survey was conducted in Ambon, Maluku, Indonesia. The distribution of apparent resistivity data from field measurements can be seen in **Fig. 7**. Based on the initial screening, the number of layers, and the search range can be determined as shown in **Table 3**. The search range/model space is selected based on graph of the resistivity and electrode spacing, then look at the pattern of decreasing or increasing the graph. From the graph also can determination of the number of layers (Koefoed, 1979).

(Table 3 here)
(Fig. 7 here)

The VFSA inversion has succeeded in obtaining model parameters that describe the subsurface conditions as shown in **Fig. 8**. The value of the objective function or misfit error from this VFSA inversion scheme is 1.58, which means that the model and field data are quite suitable and acceptable. Fitting data from model and field data can be seen in **Fig. 7**. Then the distribution of rock resistivity to depth can also be seen in **Fig. 8**.

(Fig. 8 here)
(Fig. 9 here)

The next step is to carry out a hydrogeological interpretation based on the geological conditions of the study area and the distribution of resistivity resulting from the inversion. Determination of the type of rock lithology is also based on the table of rock types and resistivity (Telford et al., 1990). Field data collection is located in the Leihitu area of Ambon City. In this area, volcanic rocks are exposed which are included in the Ambon Volcanic Rock Formation (Tpav) (**Fig 9**). Tpav was formed as a result of volcanism during the Pliocene, which spread almost throughout the Ambon region. The formation is composed of Andesite, Dacite, Breccia, and Tuff lithology (Tjokrosaputro et al., 1993).

From the sounding curve, four types of rock layers were obtained. The sounding curve represents increasing resistivity with depth but ends in conductive basal. According to the geological evaluation of the inversion results, the top layer with a resistivity of 141.2 m represents the top soil with a thickness of 1.43 meters. The layer below is andesite breccia lithology with a thickness of about 4 meters with a high resistivity of 355.9 m. The third layer with a resistivity of about 93.4 m is lapilli tuff 30 meters thick. The fourth layer is coarse tuff with a resistivity of about 34.4 m. The aquifer is estimated to be at a depth of 35.43 m and the cover layer is lapilli tuff which is characterized by a higher resistivity value. In this lithological interpretation, there is no basement layer which is usually characterized by compact rock with high resistivity values.

Based on these results, the VFSA inversion program is effective and useful for resistivity data, that application is to find groundwater potential. This program is still limited to one-dimensional resistivity data, so that further it can develop a VFSA scheme inversion program for two-dimensional or three-dimensional resistivity data.

5. CONCLUSION

The VFSA method as a type of global optimization approach for resistivity data inversion has succeeded in revealing the subsurface profile. This inversion scheme was pre-tested with synthetic data free of noise and with 5% noise to test the efficacy of this program. The inversion results show satisfactory results with a small RMSE value when using both synthetic data. To further evaluate the application of VFSA inversion, a DC-resistivity data set with a Schlumberger configuration was applied. Field data is in the form of apparent resistivity to electrode spacing, then inverse modelling is carried out to obtain model parameters in the form of rock resistivity and thickness of each layer. From the inversion results, it was found that at the measurement point there were four layers consisting of top soil (141.2 $\pm$ 0.61 m) with a thickness of 1.43 m, andesite breccia (355.90 $\pm$ 0.46 m) with a thickness of 4 m, Lapilli Tuff (93.40 $\pm$ 0.31 m) with 30 m thick, then the last Coarse Tuff layer (34.30 $\pm$ 0.15 m). The aquifer is estimated to be located from a depth of 35.43 m which is characterized by a low resistivity value with a cover layer of Lapilli Tuff rock. These results indicate the usefullness and effectiveness of the VFSA inversion scheme to be used more broadly for resistivity data, that application to find groundwater potential.

REFERENCE

Alarifi, S. S., Abdelrahman, K., & Hazaea, B. Y. (2022). Depicting of groundwater potential in hard rocks of southwestern Saudi Arabia using the vertical electrical sounding approach. *Journal of King Saud University - Science*, *34*(7), 102221. https://doi.org/10.1016/j.jksus.2022.102221

Ammar, A. I., Gomaa, M., & Kamal, K. A. (2021). Applying of SP, DC-Resistivity, DC-TDIP and TDEM soundings in high saline coastal aquifer. *Heliyon*, *7*(7), e07617. https://doi.org/10.1016/j.heliyon.2021.e07617

Bhattacharya, P. K., & Patra, H. P. (1968). *Methods in Geochemistry and Geophysics 9: Direct Current Geoelectric Sounding Electric Sounding Principles and Interpretation* (1st ed.). Elsevier Publishing Company.

Biswas, A., & Sharma, S. P. (2014). Optimization of self-potential interpretation of 2-D inclined sheet-type structures based on very fast simulated annealing and analysis

of ambiguity. *Journal of Applied Geophysics*, *105*, 235–247. https://doi.org/10.1016/j.jappgeo.2014.03.023

Chikabvumbwa, S. R., Sibale, D., Marne, R., Chisale, S. W., & Chisanu, L. (2021). Geophysical investigation of dambo groundwater reserves as sustainable irrigation water sources: case of Linthipe sub-basin. *Heliyon*, *7*(11), e08346. https://doi.org/10.1016/j.heliyon.2021.e08346

Ekinci, Y. L., & Demirci, A. (2008). A Damped Least-Squares Inversion Program for the Interpretation of Schlumberger Sounding Curves. *Journal of Applied Sciences*, *8*(22), 4070–4078. https://doi.org/10.3923/jas.2008.4070.4078

Ghosh, D. K. (1971). The Application of Linear Filter Theory to the Direct Interpretation of Geoelectrical Resistivity Sounding Measurements. *Geophysical Prospecting*, *19*(2), 192–217. https://doi.org/doi.org/10.1111/j.1365-2478.1971.tb00593.x

Guptasarma, D. (1982). optimization of short digital linear filters for increased accuracy. *Geophysical Prospecting*, *30*, 501–514.

Hapsoro, C. A., Srigutomo, W., Purqon, A., Warsa, W., Sutarno, D., & Kagiyama, T. (2021). Global inversion of grounded electric source time-domain electromagnetic data using particle swarm optimization. *Journal of Engineering and Technological Sciences*, *53*(1), 1–27. https://doi.org/10.5614/j.eng.technol.sci.2021.53.1.1

Ingber, L. (1989). Very fast simulated re-annealing. *Mathematical and Computer Modelling*, *12*(8), 967–973.

Ingber, L. (1993). Simulated annealing: practice vs theory. *Mathematical and Computer Modelling*, *18*(11), 29–57.

Joel, E. S., Olasehinde, P. I., Adagunodo, T. A., Omeje, M., Oha, I., Akinyemi, M. L., & Olawole, O. C. (2020). Geo-investigation on groundwater control in some parts of Ogun state using data from Shuttle Radar Topography Mission and vertical electrical soundings. *Heliyon*, *6*(1), e03327. https://doi.org/10.1016/j.heliyon.2020.e03327

Koefoed, O. (1979). *Geosounding Principles, 1: Resistivity Sounding Measurements* (1st ed.). Elsevier Publishing Company.

Meju, M. A. (1992). An effective ridge regression procedure for resistivity data inversion. *Computers & Geosciences*, *18*(2–3), 99–118. https://doi.org/https://doi.org/10.1016/0098-3004(92)90079-7

Narayan, S., Dusseault, M. B., & Nobes, D. C. (1994). Inversion techniques applied to resistivity inverse problems. *Inverse Problem*, *10*(3), 669.

Özyıldırım, Ö., Demirci, İ., Gündoğdu, N. Y., & Candansayar, M. E. (2020). Two dimensional joint inversion of direct current resistivity and radiomagnetotelluric data based on unstructured mesh. *Journal of Applied Geophysics*, *172*. https://doi.org/10.1016/j.jappgeo.2019.103885

Sen, M. K., & Stoffa, P. L. (2013). *Global Optimization Methods in Geophysical Inversion* (2ed ed.). Cambridge University Press.

Sharma, S. P. (2012). VFSARES — a very fast simulated annealing FORTRAN program for interpretation of 1-D DC resistivity sounding data from various electrode arrays. *Computers and Geosciences*, *42*, 177–188. https://doi.org/10.1016/j.cageo.2011.08.029

Srigutomo, W., Hapsoro, C. A., Purqon, A., Warsa, Sutarno, D., & Kagiyama, T. (2021). Nonlinear Inversion Using Very Fast Simulated Annealing for Horizontal Electric Dipole Time-Domain Electromagnetic Data. *Journal of Electromagnetic Engineering and Science*, *21*(5), 379–390. https://doi.org/10.26866/jees.2021.5.r.46

Steiner, M., Katona, T., Fellner, J., & Flores Orozco, A. (2022). Quantitative water content estimation in landfills through joint inversion of seismic refraction and electrical resistivity data considering surface conduction. *Waste Management*, *149*, 21–32. https://doi.org/10.1016/j.wasman.2022.05.020

Telford, W. M., Geldart, L. P., & Sheriff, R. E. (1990). *Applied Geophysics* (2nd ed.). Cambridge University Press.

Tjokrosaputro, S., Rusmana, E., & Achdan, A. (1993). *Peta geologi lembar ambon, maluku*. Pusat penelitian dan pengembangan geologi.

Tjong, T., Roodhiyah, L. Y., Nurhasan, & Sutarno, D. (2018). Two Dimensional Finite

Element Based Magnetotelluric Inversion using Singular Value Decomposition Method on Transverse Electric Mode. *Journal of Physics: Conference Series*, *1011*(1). https://doi.org/10.1088/1742-6596/1011/1/012042

Wang, Y., Wang, H., Wu, X., Chen, K., Liu, S., & Deng, X. (2021). Near-surface velocity inversion from Rayleigh wave dispersion curves based on a differential evolution simulated annealing algorithm. *Artificial Intelligence in Geosciences*, *2*(September), 35–46. https://doi.org/10.1016/j.aiig.2021.10.001

Wilopo, W., Risanti, Susanto, R., & Putra, D. P. E. (2018). Seawater intrusion assesment and prediction of sea-freshwater interface in Parangtritis coastal aquifer, South of Yogyakarta Special Province. *J. Degrade. Min. Land Manage*, *8*(3), 2709–2718. https://doi.org/doi:10.15243/jdmlm.2021.083.2709

Yan, L., Shen, Q., Lu, H., Wang, H., Fu, X., & Chen, J. (2020). Inversion and uncertainty assessment of ultra-deep azimuthal resistivity logging-while-drilling measurements using particle swarm optimization. *Journal of Applied Geophysics*, *178*, 104059. https://doi.org/10.1016/j.jappgeo.2020.104059

Zaher, M. A., Younis, A., Shaaban, H., & Mohamaden, M. I. I. (2021). Integration of geophysical methods for groundwater exploration: A case study of El Sheikh Marzouq area, Farafra Oasis, Egypt. *Egyptian Journal of Aquatic Research*, *47*(2), 239–244. https://doi.org/10.1016/j.ejar.2021.03.001

Table 1. True and obtained model parameters for three-layer-QQ-type model without noise

Parameters	Actual Value	Search range	Mean Model (VFSA) RMSE=0.00	Earth model (SVD) RMSE=2.86
$\rho_1\ (\Omega.\mathrm{m})$	100	(50-100)	100.00 ± 0.00	100.01
$\rho_2\ (\Omega.\mathrm{m})$	50	(20-80)	50.00 ± 0.00	50.08
$\rho_3\ (\Omega.\mathrm{m})$	20	(10-30)	20.00 ± 0.00	20.00
$h_1(m)$	5	(2-8)	5.00 ± 0.00	4.99
$h_2(m)$	10	(5-15)	10.00 ± 0.00	9.99

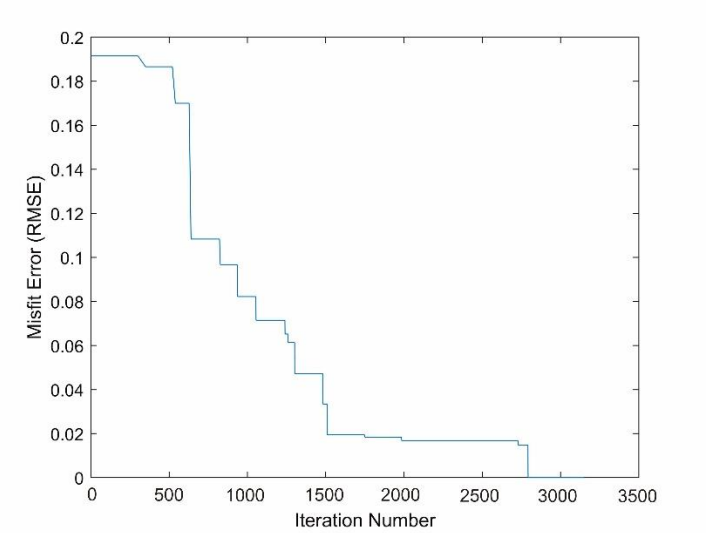

Figure. 1. Pattern of RMS eror convergence for VFSA solution with free noise data

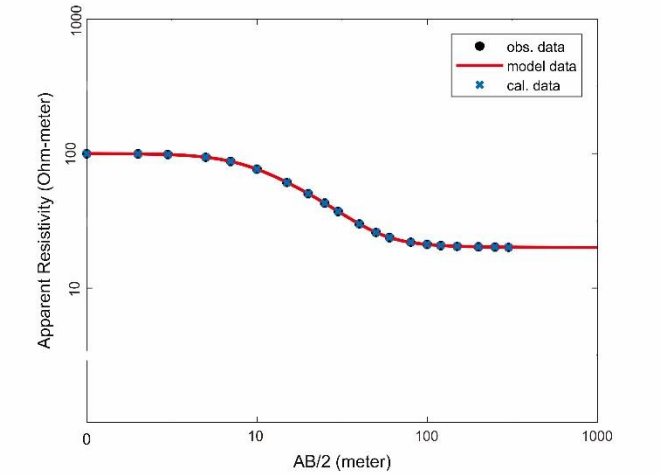

Figure 2. Apparent resistivity curves from FVSA inversion scheme result with free noise data

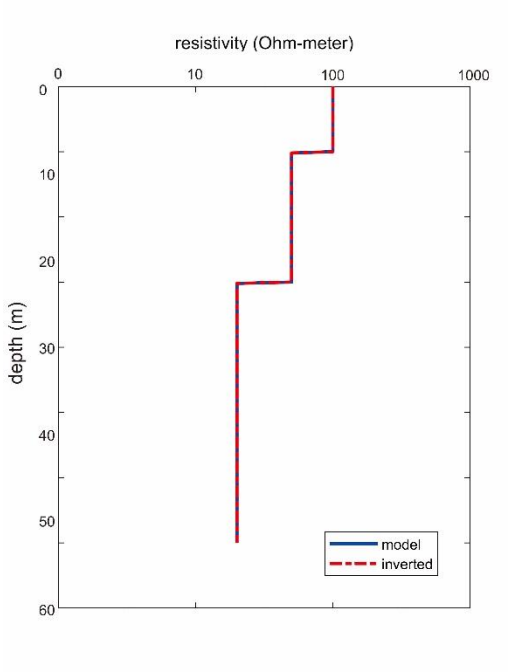

Figure 3. Resistivity-depth distribution from FVSA inversion scheme result with free noise data and true model

Table 2. True and obtained model parameters for four-layer-QQ-type model with noise 5%

Parameters	Actual Value	Search range	Mean Model (VFSA) RMSE=0.0416	Earth model (SVD) RMSE=2.86
ρ_1 (Ω.m)	100	(50-100)	100.00 ± 0.00	100.00
ρ_2 (Ω.m)	50	(20-80)	51.80 ± 0.13	51.72
ρ_3 (Ω.m)	20	(10-30)	23.00 ± 0.67	21.73
ρ_4 (Ω.m)	10	(5-15)	10.00 ± 0.00	10.07
h_1 (m)	5	(2-8)	5.00 ± 0.00	4.77
h_2 (m)	10	(5-15)	8.40 ± 0.27	9.07
h_3 (m)	20	(10-30)	19.60 ± 0.4	19.57

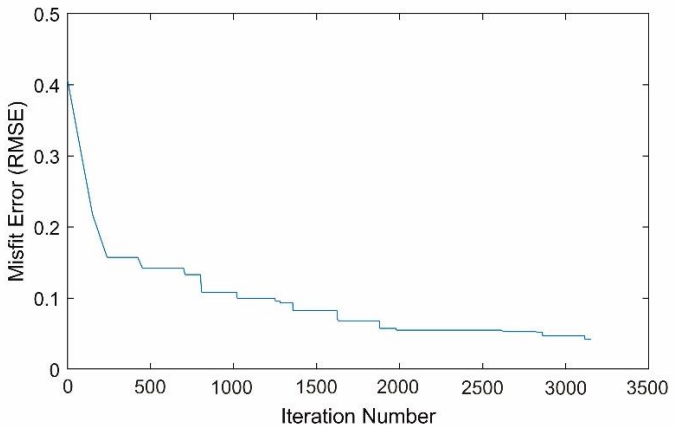

Figure 4. Pattern of the RMS eror convergence for VFSA solution with 5% noise data

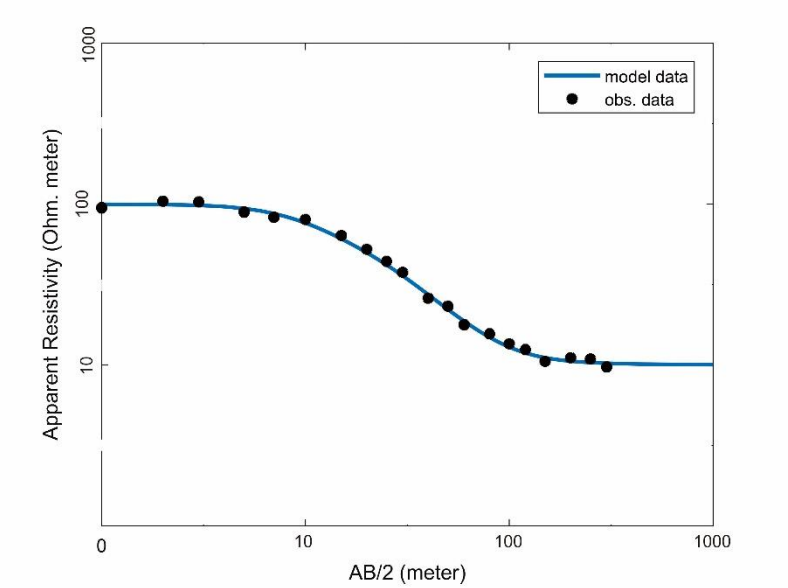

Figure 5. Apparent resistivity curves from FVSA inversion scheme result with 5% noise data

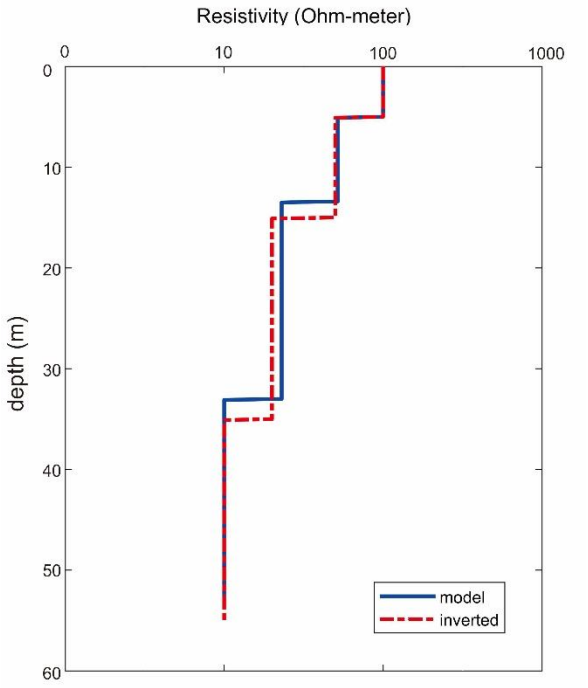

Figure 6. Resistivity-depth distribution from FVSA inversion scheme result with 5% noise data and true model

Table 3. Parameter models of the Field Data

Parameters	Search range	Inversion Result (RMSE = 1.58)	Geology Interpretation
	(100-150)		Top Soil
ρ_1 (Ω.m)		141.2.00 ± 0.61	Andesite Breccia
ρ_2 (Ω.m)	(300-400)	355.90 ± 0.46	Lapilli Tuff
ρ_3 (Ω.m)	(75-125)	93.40 ± 0.31	Coarse Tuff
ρ_4 (Ω.m)	(20-60)	34.30 ± 0.15	Top Soil
h_1 (m)	(1-5)	1.43 ± 0.02	Andesite Breccia
h_2 (m)	(1-10)	4.00 ± 0.00	Lapilli Tuff
h_3 (m)	(10-30)	30.00 ± 0.00	

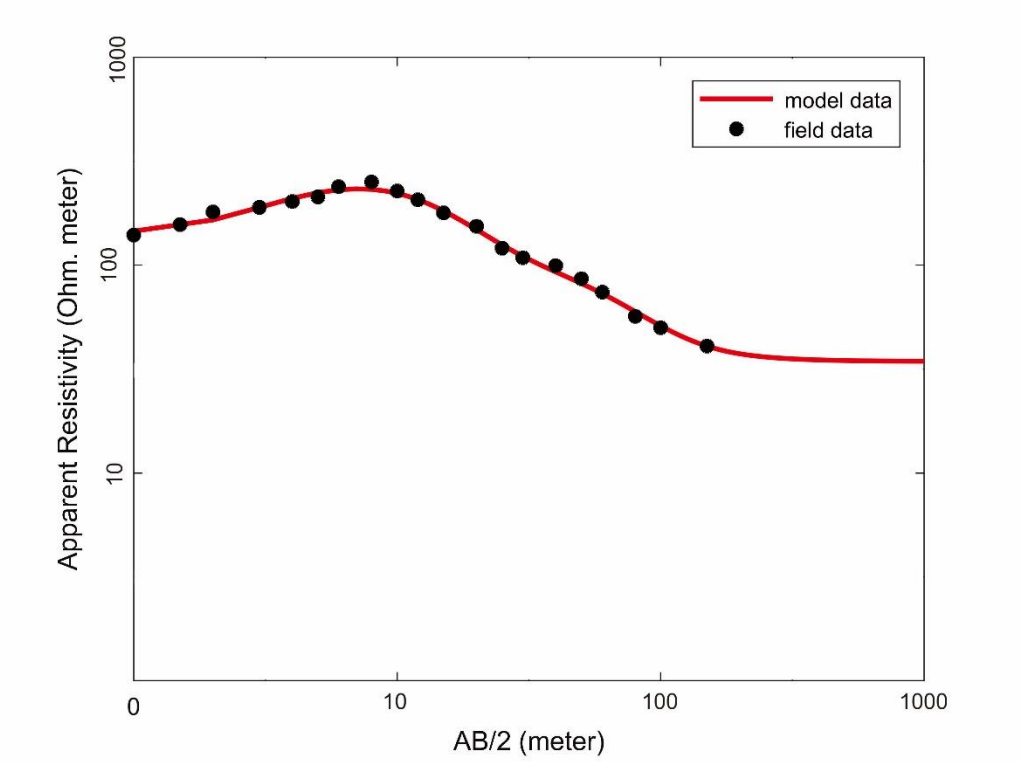

Figure 7. Observed and calculated apparent resistivity curves for the field data

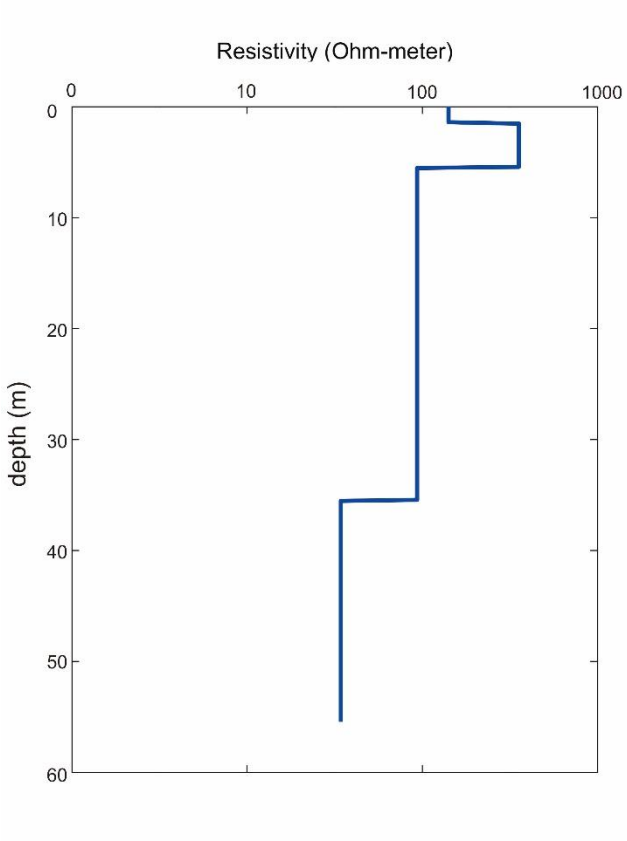

Figure 8. Inverted subsurface resistivity model from the VFSA inversion scheme for the field data

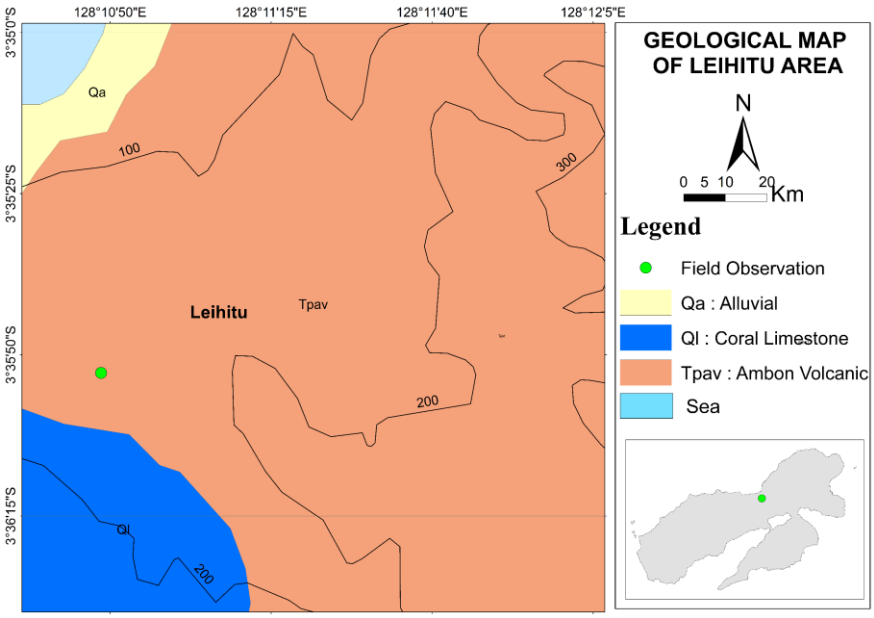

Figure 9. Geological map of Leihitu Area (Modification from Tjokrosapoetro et. al., 1993)

19% Overall Similarity

Top sources found in the following databases:

- 10% Internet database
- Crossref database
- 7% Submitted Works database
- 17% Publications database
- Crossref Posted Content database

TOP SOURCES

The sources with the highest number of matches within the submission. Overlapping sources will not be displayed.

1	jees.kr Internet	5%
2	Madan K. Jha, S. Kumar, A. Chowdhury. "Vertical electrical sounding s... Crossref	3%
3	Sharma, S.P.. "VFSARES-a very fast simulated annealing FORTRAN pro... Crossref	1%
4	Yunus Levent Ekinci, Alper Demirci. "A Damped Least-Squares Inversio... Crossref	1%
5	Indian School of Mines on 2018-10-12 Submitted works	<1%
6	Sylvester Richard Chikabvumbwa, Davis Sibale, Ramadan Marne, Sylve... Crossref	<1%
7	library.seg.org Internet	<1%
8	Wahyu Srigutomo, Cahyo Aji Hapsoro, Acep Purqon, Warsa, Doddy Sut... Crossref	<1%

9	Indian Institute of Technology, Bombay on 2019-02-18 Submitted works	<1%
10	citeseerx.ist.psu.edu Internet	<1%
11	Indian School of Mines on 2020-01-12 Submitted works	<1%
12	S.P. Sharma. "Appraisal of equivalence and suppression problems in 1... Crossref	<1%
13	academic.oup.com Internet	<1%
14	link.springer.com Internet	<1%
15	dalerucker.com Internet	<1%
16	Arkoprovo Biswas. "Inversion of Source Parameters from Magnetic An... Crossref	<1%
17	Botswana International University of Science and Technology on 2020-... Submitted works	<1%
18	Indian School of Mines on 2020-05-02 Submitted works	<1%
19	M.A Meju, P.J Fenning, T.R.W Hawkins. "Evaluation of small-loop trans... Crossref	<1%
20	Nazifi, Hafiz Mohammed. "The Use of Integrated Geophysical Methods... Publication	<1%

21	School of Business and Management ITB on 2019-08-27 Submitted works	<1%
22	University of Luton on 2009-01-14 Submitted works	<1%
23	University of Zululand on 2018-07-30 Submitted works	<1%
24	dora.dmu.ac.uk Internet	<1%
25	m.scirp.org Internet	<1%
26	scholar.ufs.ac.za Internet	<1%
27	Shashi Prakash Sharma, Arkoprovo Biswas. "Interpretation of self-pote... Crossref	<1%
28	Wahyu Srigutomo, Cahyo Aji Hapsoro, Acep Purqon, Warsa, Doddy Sut... Crossref	<1%
29	Akmam, H Amir, A Putra, R Anshari, N Jalinus. "Implementation of leas... Crossref	<1%